

# HIGH-ORDER PERTURBATION SOLUTIONS TO A LH<sub>2</sub> SPREADING MODEL WITH CONTINUOUS SPILL

Kim, M.<sup>1</sup>, Do, K.<sup>2</sup>, Choi, B.<sup>3</sup>, Han, Y.<sup>4</sup>

<sup>1</sup> Division of Plant Safety and Reliability, Korea Institute of Machinery & Materials, 104 Shinsung-no, Yusong, Daejeon, 305-343, South Korea, mbkim@kimm.re.kr

<sup>2</sup> Division of Plant Safety and Reliability, Korea Institute of Machinery & Materials, 104 Shinsung-no, Yusong, Daejeon, 305-343, South Korea, kyudo@kimm.re.kr

<sup>3</sup> Division of Plant Safety and Reliability, Korea Institute of Machinery & Materials, 104 Shinsung-no, Yusong, Daejeon, 305-343, South Korea, cbisey@kimm.re.kr

<sup>4</sup> Division of Plant Safety and Reliability, Korea Institute of Machinery & Materials, 104 Shinsung-no, Yusong, Daejeon, 305-343, South Korea, yshan@kimm.re.kr

## ABSTRACT

High-order perturbation solutions have been obtained for the simple physical model describing the LH<sub>2</sub> spreading with a continuous spill, and are shown to improve over the first-order perturbation solutions. The non-dimensional governing equations for the model are derived to obtain more general solutions. Non-dimensional parameters are sought as the governing parameters for the non-dimensional equations, and the non-dimensional evaporation rate is used as the perturbation parameter. The results show that the second-order solutions exhibit an improvement over the first-order solutions with respect to the pool volume; however, there is still a difference between numerical solutions and second-order solutions in the late stage of spread. Finally, it is revealed that the third-order solutions almost agree with numerical solutions.

## NOMENCLATURE

$E$  : evaporation rate per unit area (m/s)

$g$  : gravity (m/s<sup>2</sup>)

$H$  : pool height (m)

$h$  : dimensionless pool height

$L$  : characteristic length(m)

$R$  : pool radius (m)

$r$  : dimensionless pool radius

$T$  : time(s)

$t$  : dimensionless time

$V$  : pool volume(m<sup>3</sup>)

$V$  : dimensionless pool volume

$\alpha$  :  $2g\Delta$  (m/s<sup>2</sup>)

$\beta$  : spill source rate(m<sup>3</sup>/s)

$\varepsilon$  : dimensionless evaporation rate

$\Delta$  : 1 for spread on the ground and  $1-\rho/\rho_w$  for spread on the water

$\rho$  : density of fluid(kg/m<sup>3</sup>)

$\rho_w$  : density of water(kg/m<sup>3</sup>)

$\tau$  : characteristic time (s)

### **Subscripts**

$i$  : initial value

$0$  : zeroth-order term

$1$  : first-order term

$2$  : second-order term

$3$  : third-order term

## **1. INTRODUCTION**

The study of liquid pool spreading plays an essential role in the quantitative risk assessment of accidentally released cryogenic liquids, such as LNG and liquefied hydrogen because the spreading of such liquids is the first step in the development of multi-staged accident sequences leading to a major disaster.

A number of numerical simulations have been performed for certain model equations governing the pool spread. Various types of governing equations, ranging from a simple physical model to the full Navier-Stokes equation[1], are available for numerical simulations. The model based on shallow layer equations[2-7] under the assumption of axisymmetry, solves for the velocity and pool height with respect to radius and time. The simplest mathematical model, which can be called the simple physical model[7] describes the pool spread in terms of how the pool radius and height evolve in time. The corresponding equations consist of two ordinary differential equations with respect to time and one algebraic equation. For the purpose of engineering design and analysis, however, the shallow layer model presents a problem in determining the size of the pool fire because the model allows the leading-edge wave to separate from the spreading pool to form an annulus.

In this study, a set of third-order perturbation solutions are derived, as an improvement over the previous first-order perturbation solutions[8], for the simple physical model describing the liquid pool spreading with a continuous spill. The third-order solutions are derived for the governing equations after introducing dimensionless governing parameters in order to obtain generic solutions. The normalized, dimensionless evaporation rate per unit area is used as the perturbation parameter. The results demonstrate that the second-order solutions exhibit an improvement over the first-order solutions with respect to the pool volume; however, the two types of perturbation solutions present nearly identical results for the pool radius. There is still difference between numerical solutions and second-order solutions for the pool volume in the late stage of spread even though second-order solutions improve over first-order solutions. Finally, it is revealed that the third-order solutions almost agree with numerical solutions for the pool volume.

## **GOVERNING EQUATIONS**

Neglecting the surface tension and viscous drag, the driving force for the pool spread is gravity. Although this force acts downwards, it creates an unbalanced pressure distribution in the pool, causing the pool to spread laterally. Pool spread is governed by the following set of equations[7]:

$$\frac{dR}{dT} = \sqrt{\alpha H}, \quad (1)$$

where  $R$  - pool radius, m;  $T$  - time, s;  $\alpha = 2g\Delta$ , m/s<sup>2</sup>;  $g$  - gravity, m/s<sup>2</sup>;  $\Delta = 1$  for spills on the ground or  $1 - \rho/\rho_w$  for spills on water;  $\rho$  - density of liquid, kg/m<sup>3</sup>;  $\rho_w$  - density of water, kg/m<sup>3</sup>;  $H$  - pool height, m.

$$\frac{dV}{dT} = -E\pi R^2 + \beta, \quad (2)$$

where  $V$  - pool volume, m<sup>3</sup>;  $E$  - evaporation rate per unit area, m/s;  $\beta$  - spill source rate, m<sup>3</sup>/s. Therefore, for an instantaneous spill,  $\beta$  becomes zero. To complete the model, the following algebraic equation is required:

$$H = \frac{V}{\pi R^2} \quad (3)$$

Although surface tension and viscous drag are neglected in the present study, they are usually only important for spills of a high viscosity liquid like oil on water. The effect of viscous drag can not be considered because cryogenic liquid spills vaporizes relatively quickly and rarely reach a gravity-viscous regime of pool spread[7].

## INITIAL CONDITIONS AND SOLUTIONS

If the liquid is continuously released from storage, the following initial conditions can be used:

$$V(0) = 0, \quad R(0) = 0 \quad H(0) = 0 \quad (4)$$

From Eq. 1 through 4 it is understood that the evaporation rate per unit area,  $E$ , and the spill source rate,  $\beta$ , govern the model equations for the spread on the ground. For simplicity, the spread on the ground is considered in the present study. To make the governing equations dimensionless, the following variables are introduced:

$$v = \frac{V}{\pi L^3}, \quad r = \frac{R}{L}, \quad h = \frac{H}{L}, \quad t = \frac{T}{\tau}, \quad (5)$$

where  $v$  - dimensionless volume;  $r$  - dimensionless radius;  $h$  - dimensionless height;  $t$  - dimensionless time;  $\tau$  and  $L$  are the characteristic time and length scale defined by:

$$\tau = \left( \frac{\beta}{\alpha^3} \right)^{1/5}, \quad L = \left( \frac{\beta^2}{\alpha} \right)^{1/5} \quad (6)$$

Using the dimensionless variables in Eq. 5, the following non-dimensional governing equations are derived:

$$\frac{dv}{dt} = \frac{1}{\pi} - \varepsilon r^2, \quad (7)$$

where  $\varepsilon$  - dimensionless evaporation rate,  $\tau E/L$ .

$$\frac{dr}{dt} = \sqrt{h} \quad (8)$$

$$h = \frac{v}{r^2} \quad (9)$$

From Eq. 7 through 9 it can be seen that the dimensionless number,  $\varepsilon$ , corresponding to the dimensionless evaporation rate per unit area, is the unique parameter which can control the non-dimensional governing equations. The initial conditions are

$$v = 0, \quad r = 0, \quad h = 0 \quad \text{at} \quad t = 0 \quad (10)$$

The evaporation rate per unit area of LH<sub>2</sub> on a paraffin wax ground[4] varies from about  $4.23 \times 10^{-4}$  m/s to about  $12.7 \times 10^{-4}$  m/s. Therefore, the dimensionless evaporation rate,  $\varepsilon$ , can be chosen as the perturbation parameter. The perturbation solutions can then be expressed in the following forms:

$$v = v_0 + \varepsilon v_1 + \varepsilon^2 v_2 + \varepsilon^3 v_3, \quad (11)$$

where  $v_0$  - zeroth order term,  $v_1$  - 1st order term,  $v_2$  - 2nd order term,  $v_3$  - 3rd order term.

$$r = r_0 + \varepsilon r_1 + \varepsilon^2 r_2 + \varepsilon^3 r_3, \quad (12)$$

where  $r_0$  - zeroth order term,  $r_1$  - 1st order term,  $r_2$  - 2nd order term,  $r_3$  - 3rd order term.

$$h = h_0 + \varepsilon h_1 + \varepsilon^2 h_2 + \varepsilon^3 h_3, \quad (13)$$

where  $h_0$  - zeroth order term,  $h_1$  - 1st order term,  $h_2$  - 2nd order term,  $h_3$  - 3rd order term.

Terms higher than  $O(\varepsilon^3)$  are omitted. In this study, a third-order expansion is used, and terms up to  $O(\varepsilon^3)$  are retained. Substituting Eq. 11 through 13 into Eq. 7 through 9 and equating the coefficients of  $\varepsilon^0$ ,  $\varepsilon$ ,  $\varepsilon^2$  and  $\varepsilon^3$  on both-hand sides, we obtain

$$\frac{dr_0}{dt} = \sqrt{h_0} \quad (14)$$

$$\frac{dr_1}{dt} = \frac{h_1}{2\sqrt{h_0}} \quad (15)$$

$$\frac{dr_2}{dt} = \frac{h_2}{2\sqrt{h_0}} \quad (16)$$

$$\frac{dr_3}{dt} = \frac{h_3}{2\sqrt{h_0}} \quad (17)$$

$$\frac{dv_0}{dt} = \frac{1}{\pi} \quad (18)$$

$$\frac{dv_1}{dt} = -r_0^2 \quad (19)$$

$$\frac{dv_2}{dt} = -2r_0 r_1 \quad (20)$$

$$\frac{dv_3}{dt} = -r_1^2 - 2r_0 r_2 \quad (21)$$

$$h_0 = \frac{v_0}{r_0^2} \quad (22)$$

$$h_1 = \frac{v_1}{r_0^2} \quad (23)$$

$$h_2 = \frac{v_2}{r_0^2} \quad (24)$$

$$h_3 = \frac{v_3}{r_0^2} \quad (25)$$

Twelve new equations (Eq. 14 through 25) have been obtained; therefore, the number of initial conditions must increase to twelve. Applying the conditions in Eq. 10 to Eq. 11 through 13 and equating the coefficients of  $\varepsilon^0$ ,  $\varepsilon$  and etc. on both sides, we get

$$v_0 = 0, \quad r_0 = 0, \quad h_0 = 0 \quad \text{at } t=0 \quad (26)$$

$$v_1 = 0, \quad r_1 = 0, \quad h_1 = 0 \quad \text{at } t=0 \quad (27)$$

$$v_2 = 0, \quad r_2 = 0, \quad h_2 = 0 \quad \text{at } t=0 \quad (28)$$

$$v_3 = 0, \quad r_3 = 0, \quad h_3 = 0 \quad \text{at } t=0 \quad (29)$$

Solving Eq. 14 through 25 with the initial conditions in Eq. 26 through 29 yields

$$r_0 = \frac{2}{\sqrt{3}} \left( \frac{1}{\pi} \right)^{1/4} t^{3/4} \quad (30)$$

$$r_1 = -\frac{8\sqrt{3}}{135} \pi^{1/4} t^{9/4} \quad (31)$$

$$r_2 = \frac{8\sqrt{3}}{2025} \pi^{3/4} t^{15/4} \quad (32)$$

$$r_3 = \frac{64\sqrt{3}}{280665} \pi^{5/4} t^{21/4} \quad (33)$$

And

$$v_0 = \frac{t}{\pi} \quad (34)$$

$$v_1 = -\frac{8}{15\sqrt{\pi}} t^{5/2} \quad (35)$$

$$v_2 = \frac{8}{135}t^4 \quad (36)$$

$$v_3 = -\frac{64\sqrt{\pi}}{13365}t^{11/2} \quad (37)$$

$$h_0 = \frac{3}{4\sqrt{\pi}}\frac{1}{\sqrt{t}} \quad (38)$$

$$h_1 = -\frac{2}{5}t \quad (39)$$

$$h_2 = \frac{2\sqrt{\pi}}{45}t^{5/2} \quad (40)$$

$$h_3 = -\frac{16\pi}{4455}t^4 \quad (41)$$

## RESULTS AND DISCUSSION

For the purpose of numerical evaluation, a spreading of LH<sub>2</sub> on the paraffin wax with the values of  $E = 4.2 \times 10^{-4}$  m/s has been considered. The result[8] for the pool volume is shown in Fig. 1, in which the difference between the numerical solution and the first-order solution becomes evident in the late stage of spread when the time is large. This discrepancy comes from the secular terms[9] that lead to the non-uniform expansion when time is large.

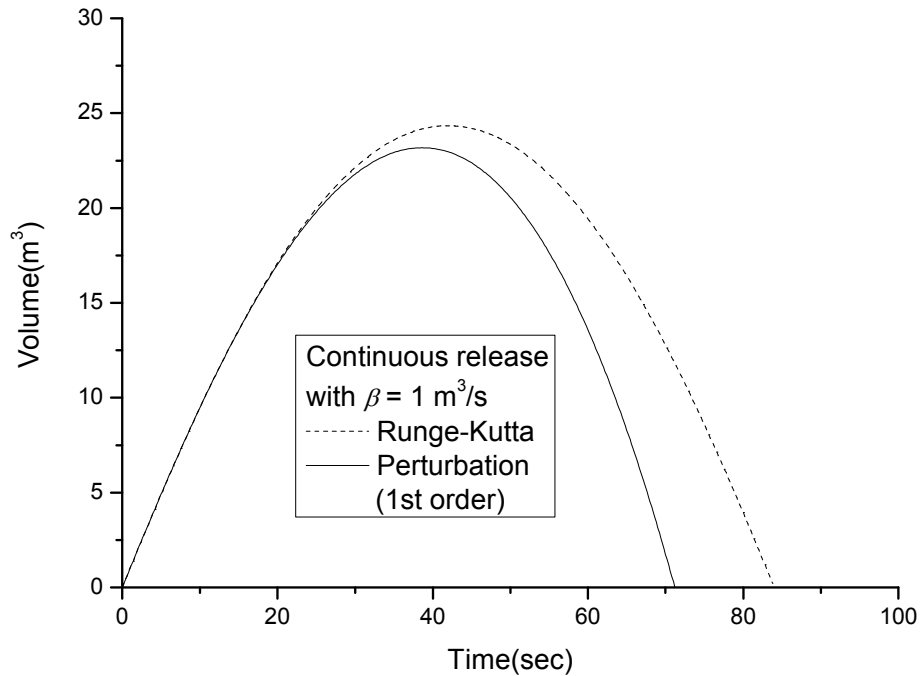


Figure 1. The pool volume vs. time

From Eqs. 34 and 35, the first-order expansion for the dimensionless pool volume can be expressed as

$$v = \frac{t}{\pi} - \varepsilon \frac{8}{15\sqrt{\pi}} t^{5/2} \quad (42)$$

or in dimensional terms,

$$V = \beta T - E \frac{8}{15} \sqrt{\pi \alpha \beta} T^{5/2} \quad (43)$$

In Eq. 43, the second term should be much smaller than the first term because the second term has been introduced as the correction term for the first term. As time increases, however, the order of the correction term,  $O(ET^{5/2})$ , approaches  $O(1)$ . That is, the correction term becomes of the order of the main term for a large  $T$ . To address this anomaly, a uniform expansion would be adequate; however, it is beyond the scope of the present study. Instead, the higher order expansion has been pursued.

The second-order and third-order solutions have been calculated for the spill source rate of  $10^{-2} \text{ m}^3/\text{s}$ ,  $10^0 \text{ m}^3/\text{s}$ , and  $10^2 \text{ m}^3/\text{s}$  in order to explore the effect of the unique governing parameter on the solutions. In the case of the pool volume, as seen in Fig. 2-4, the second-order solutions exhibit an improvement over the first-order solutions; however, there are still differences between numerical solutions and second-order solutions in the late stage of spread. It can be known that third-order solutions approximate to the numerical solutions for all stages of spread. It is shown that the perturbation solutions generally allow for a change in the spill source rate.

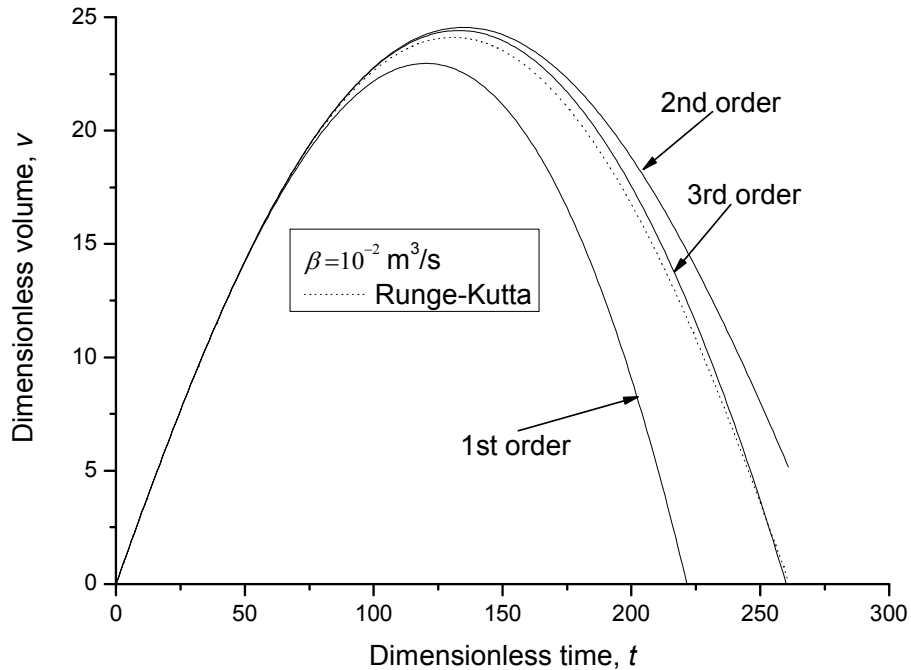


Figure 2. Dimensionless volume vs. dimensionless time with  $\beta=10^{-2} \text{ m}^3/\text{s}$

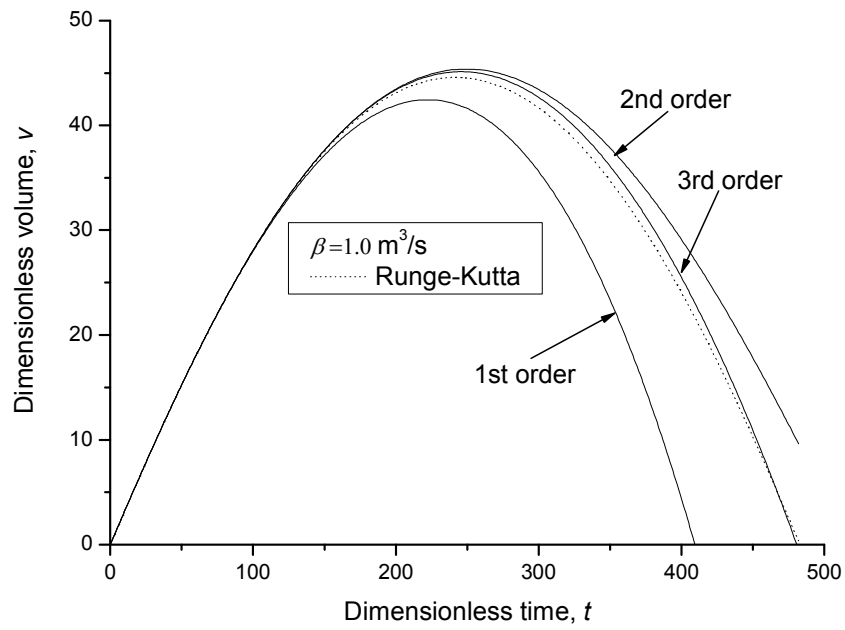


Figure 3. Dimensionless volume vs. dimensionless time with  $\beta=10^0 \text{ m}^3/\text{s}$

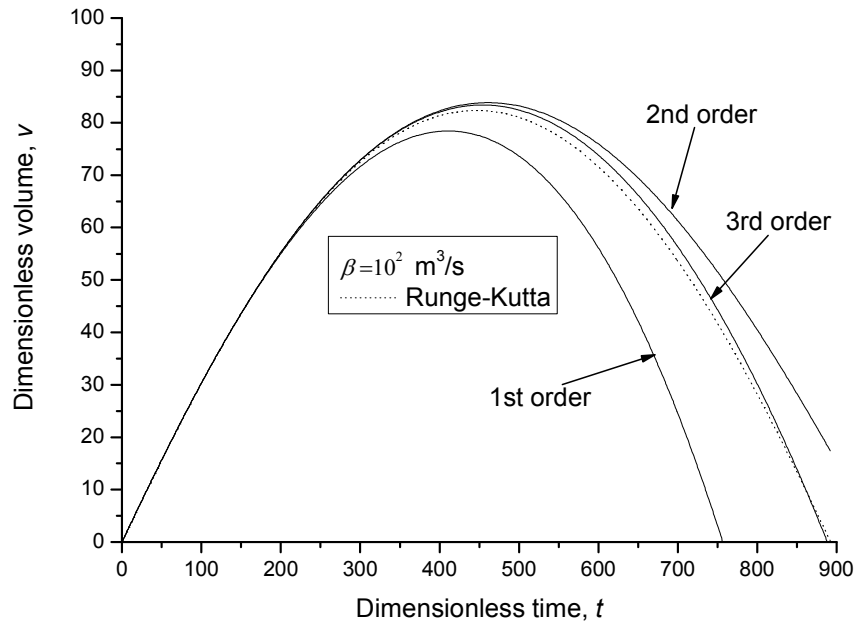


Figure 4. Dimensionless volume vs. dimensionless time with  $\beta=10^2 \text{ m}^3/\text{s}$

For the radius as can be seen in Fig. 5-7, the third-order and second order solutions are identical except the far late stage of spread when the time is very large. The high-order solutions display an improvement over the first-order solutions except the far late stage of spread and the three perturbation



solutions are indistinguishable in the early stage. There are still differences between numerical solutions and high-order solutions when the time is very large. Increase of the spill source rate,  $\beta$ , decreases the differences at the same time because increase of the spill source rate decreases the non-dimensional evaporation rate,  $\varepsilon$ , which leads to keep the correction terms (Eq. 31 to 33) small in spite of the relatively large values of time. The results also demonstrate that the high-order perturbation solutions readily accommodate the change in the unique parameter.



Figure 5. Dimensionless radius vs. dimensionless time with  $\beta=10^{-2} \text{ m}^3/\text{s}$

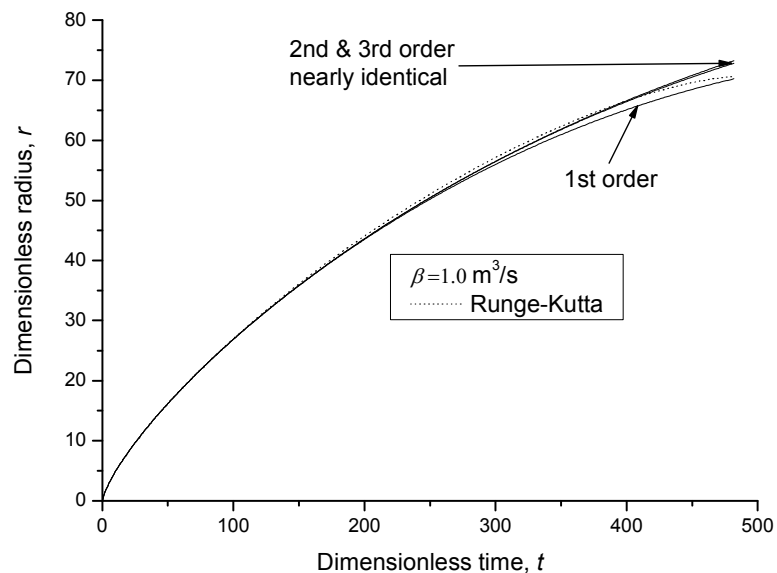


Figure 6. Dimensionless radius vs. dimensionless time with  $\beta=10^0 \text{ m}^3/\text{s}$

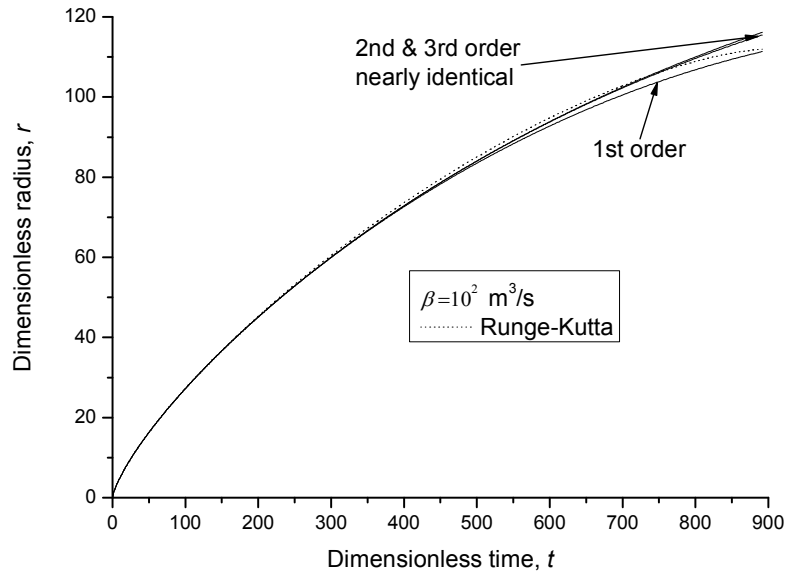


Figure 7. Dimensionless radius vs. dimensionless time with  $\beta=10^2 \text{ m}^3/\text{s}$

The mathematical form of the spreading model is the nonlinear simultaneous differential equations. These equations were solved numerically in the past. However, the present study is to solve these equations analytically. Perturbation methods are used to solve the equations in this work. Using the mathematical techniques closed-form solutions that are mathematically complete can be obtained. Therefore it can be said that perturbation methods are quite different from generic numerical simulation.

## CONCLUSION

The model equations for the spread of a liquid pool with continuous spill have been made dimensionless to reveal that these equations are governed by one parameter, namely, the dimensionless evaporation rate. It is noteworthy that the original governing equations, before being made dimensionless, contain two governing parameters instead of one.

For the dimensionless governing equations, the high-order perturbation solutions are obtained. It is found that the second-order solutions moderately improve the first-order solutions with respect to the pool volume; however, there are still differences between numerical solutions and the second-order solutions in the late stage of spread. The third-order solutions approximate to the numerical solutions for all stages of spread. For the pool radius the third-order and second order solutions are identical except the far late stage of spread when the time is very large. The high-order solutions display an improvement over the first-order solutions except the far late stage of spread and the three perturbation solutions are indistinguishable in the early stage. There are still differences between numerical solutions and high-order solutions when the time is very large. All perturbation solutions readily accommodate changes in the unique parameter. It is found that the increase of the spill source rate can keep the correction terms of perturbation solutions small even if time increases.

## REFERENCES

1. Venetsanos, A. G. and Bartzis, J. G., CFD modeling of large-scale LH2 spills in open environment, 1<sup>st</sup> International Conference on Hydrogen Safety, Pisa, Italy, 2005, pp. 125-136.
2. Stein, W. and Ermak, D. L., One-dimensional numerical fluid dynamics model of the spreading of liquefied gaseous fuel(LGF) on water, Lawrence Livermore National Laboratory Report No.UCRL-53078, 1980.
3. Verfondern, K. and Dienhart, B., Experimental and theoretical investigation of liquid hydrogen pool spreading and vaporization, Int J Hydrogen Energy, 25, 1997, pp. 649-660.
4. Verfondern, K. and Dienhart, B., Pool spreading and vaporization of liquid hydrogen, Int J Hydrogen Energy, 32, 2007, pp. 256-267.
5. Brandeis, J. and Kansa, E., Numerical simulation of liquefied fuel spills: I. Instantaneous release into a confined area, Int J Numer Methods Fluids, 3, 1983, pp. 333-345.
6. Brandeis, J. and Ermak, D., Numerical simulation of liquefied fuel spills: II. Instantaneous and continuous LNG spills on an unconfined water surface, Int J Numer Methods Fluids, 3, 1983, pp. 347-361.
7. Briscoe, F. and Shaw, P., Spread and evaporation of liquid, Progr Energy Comb Sci, 6, 1980, pp. 127-140.
8. Kim, M., Do, K., Choi, B. and Han, Y., First-order perturbation solutions of liquid pool spreading with vaporization, Int J Hydrogen Energy, 36, 2011, pp. 3268-3271.
9. Nayfeh, A., Introduction to perturbation techniques, John Wiley and Sons, New York, 1981, p.113.